

# Simulation analysis of the effects of a back surface field on a p-a-Si:H/n-c-Si/n<sup>+</sup>-a-Si:H heterojunction solar cell\*

Hu Yuehui(胡跃辉)<sup>†</sup>, Zhang Xiangwen(张祥文), Qu Minghao(曲铭浩), Wang Lifu(王立富),  
Zeng Tao(曾涛), and Xie Yaojiang(谢耀江)

(Jingdezhen Ceramics Institution, Jingdezhen 333001, China)

**Abstract:** In order to investigate the effects of a back surface field (BSF) on the performance of a p-doped amorphous silicon (p-a-Si:H)/n-doped crystalline silicon (n-c-Si) solar cell, a heterojunction solar cell with a p-a-Si:H/n-c-Si/n<sup>+</sup>-a-Si:H structure was designed. An n<sup>+</sup>-a-Si:H film was deposited on the back of an n-c-Si wafer as the BSF. The photovoltaic performance of p-a-Si:H/n-c-Si/n<sup>+</sup>-a-Si:H solar cells were simulated. It was shown that the BSF of the p-a-Si:H/n-c-Si/n<sup>+</sup>-a-Si:H solar cells could effectively inhibit the decrease of the cell performance caused by interface states.

**Key words:** p-n-n<sup>+</sup> solar cell; heterojunction; back surface field; computer simulation

**DOI:** 10.1088/1674-4926/30/6/064006

**PACC:** 6140; 6855

## 1. Introduction

Recently, scientists have made tremendous efforts on low-cost, high-efficiency solar cells, and many important results have been achieved<sup>[1]</sup>. Using the energy band project, Zhu *et al.* investigated the na-Si/c-Si solar cell, achieved a stable efficiency of 17.27% and making some fairly good attempt at creating a low-cost, high-efficiency solar cell. However, for the heterojunction solar cell, owing to the effect of interface defect state on the solar cell performance, a large amount of work should be carried out on improving the cell efficiency. In this paper, in order to investigate the effects of a back surface field (BSF) on the performance of a p-doped amorphous silicon(p-a-Si:H)/n-doped crystalline silicon (n-c-Si) solar cell, a heterojunction solar cell with a p-a-Si:H/n-c-Si/n<sup>+</sup>-a-Si:H (p-n-n<sup>+</sup>) structure, as shown in Fig. 1, was designed by the energy band project. In this structure, an n<sup>+</sup>-a-Si:H film was deposited on the back of an n-c-Si wafer as the BSF. The photovoltaic performance of a p-a-Si:H/n-c-Si solar cell and a p-a-Si:H/n-c-Si/n<sup>+</sup>-a-Si:H solar cell were simulated by AMPS-1D, respectively.

## 2. Device modeling

For the modeling calculations discussed in the following section, the software AMPS-1D was used. It can calculate the steady-state band diagram, the recombination profile, the carrier transport in one dimension based on the Poisson equation, and the hole and electron continuity equations. They are given, respectively, by<sup>[2]</sup>

$$\frac{d}{dx} \left( \varepsilon(x) \frac{d\psi}{dx} \right) = q[p(x) - n(x) + N_D^+(x) - N_A^-(x) + p_t(x) - n_t(x)], \quad (1)$$

where the electrostatic potential  $\psi$ , the free electron and hall

concentrations  $n$  and  $p$ , trapped electron and hole concentrations  $n_t$  and  $p_t$ , the ionized donor-like doping  $N_D^+$  and ionized acceptor-like doping  $N_A^-$  concentrations are all functions of the position coordinate  $x$ . Here,  $\varepsilon$  is the permittivity and  $q$  is the magnitude of the charge of one electron.

$$\frac{1}{q} \left( \frac{dJ_n}{dx} \right) = -G_{op}(x) + R(x), \quad (2)$$

$$\frac{1}{q} \left( \frac{dJ_p}{dx} \right) = G_{op}(x) - R(x), \quad (3)$$

Equations (2) and (3) include the term  $G_{op}(x)$ , which is the optical generation rate as a function of  $x$ , and  $G_{op}(x)$  is expressed as

$$G_{op}(x) = -\frac{d}{dx} \sum_i \Phi_i^{FOR}(\lambda_i) + \frac{d}{dx} \sum_i \Phi_i^{REV}(\lambda_i),$$

where  $\Phi_i^{FOR}(\lambda_i)$  and  $\Phi_i^{REV}(\lambda_i)$  are, respectively, the photon flux of the incident light and the light reflected from the back surface at a wavelength of  $\lambda_i$  at some point  $x$ , depending on the light absorption coefficient, and the light reflectance in the forward and reverse direction. In our simulation, the reflection indices for the forward (RF) and reverse (RB) directions are 0 and 0.6, respectively. The term  $R(x)$  in Eqs. (2) and (3) is the carrier recombination rate.

The governing Eqs. (1), (2), and (3) must hold at every

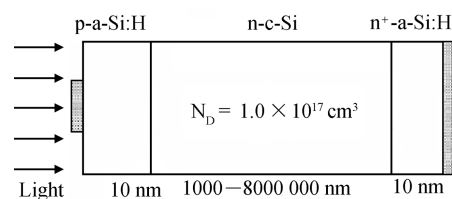


Fig. 1. Schematic of the modeling solar cell device.

\* Project supported by the Natural Science Foundation of Jiangxi Province, China (Nos. 0612025, 2007GZW0787) and the Education Bureau of Jiangxi Province, China (No. [2007]218).

<sup>†</sup> Corresponding author. Email: 8489023@163.com

Received 29 November 2008, revised manuscript received 5 February 2009

© 2009 Chinese Institute of Electronics

Table 1. Parameters used in the modeling calculation.

Parameter	p-a-Si:H	n-c-Si	n <sup>+</sup> -a-Si:H
Thickness (nm)	10	10 <sup>3</sup> –8 × 10 <sup>6</sup>	10
χ <sub>e</sub> (eV)	3.8	4.05	3.8
E <sub>G</sub> (eV)	1.8	1.12	1.8
E <sub>GOP</sub> (eV)	1.72	1.12	1.72
ε <sub>r</sub>	11.90	11.90	11.90
N <sub>C</sub> (cm <sup>-3</sup> ·eV)	2.5 × 10 <sup>20</sup>	2.8 × 10 <sup>19</sup>	2.5 × 10 <sup>20</sup>
N <sub>V</sub> (cm <sup>-3</sup> ·eV)	2.5 × 10 <sup>20</sup>	1.04 × 10 <sup>19</sup>	2.5 × 10 <sup>20</sup>
μ <sub>n</sub> (cm <sup>2</sup> /(V·s))	20	1350	20
μ <sub>p</sub> (cm <sup>2</sup> /(V·s))	2	450	2
E <sub>D</sub> , E <sub>A</sub> (eV)	0.05, 0.02	0.01, 0.01	0.05, 0.02
TSIG/N (cm <sup>-2</sup> )	1 × 10 <sup>-17</sup>	1 × 10 <sup>-17</sup>	1 × 10 <sup>-17</sup>
TSIG/P (cm <sup>-2</sup> )	1 × 10 <sup>-15</sup>	1 × 10 <sup>-15</sup>	1 × 10 <sup>-15</sup>
MSIG/N (cm <sup>-2</sup> )	1 × 10 <sup>-15</sup>	1 × 10 <sup>-15</sup>	1 × 10 <sup>-15</sup>
MSIG/P (cm <sup>-2</sup> )	1 × 10 <sup>-14</sup>	1 × 10 <sup>-14</sup>	1 × 10 <sup>-14</sup>
N <sub>A</sub> , N <sub>D</sub> (cm <sup>-3</sup> )	N <sub>A</sub> = 8 × 10 <sup>18</sup>	N <sub>D</sub> = 1 × 10 <sup>17</sup>	N <sub>D</sub> = 8 × 10 <sup>19</sup>

Note: χ<sub>e</sub> is the electron affinity; E<sub>G</sub> and E<sub>GOP</sub> are the mobility bandgap and the optical bandgap, respectively; μ<sub>n</sub> and μ<sub>p</sub> are the electron mobility and the hole mobility, respectively; N<sub>C</sub> and N<sub>V</sub> are the effective density of states in the conduction band and valence band, respectively; ε<sub>r</sub> is the relative permittivity; E<sub>D</sub> and E<sub>A</sub> are characteristic energies for donor-like tails and acceptor-like tails, respectively; TSIG/N and TSIG/P are capture cross sections for electrons and holes in tail states, respectively; MSIG/N and MSIG/P are capture cross sections for electrons and holes in midgap states, respectively; N<sub>A</sub> and N<sub>D</sub> are doping concentration of acceptor and donor, respectively.

position in a device, and the solution to these equations involves determining the state variables Ψ(x), the n-type quasi-Fermi level E<sub>Fn</sub>, and the p-type quasi-Fermi level E<sub>Fp</sub> or, equivalently, Ψ(x), n(x), and p(x), which completely defines the system at every point x. Because the governing equations for Ψ(x), E<sub>Fn</sub>, and E<sub>Fp</sub> are non-linear and coupled, they cannot be solved analytically. These must be boundary conditions imposed on the set of equations. The Newton-Raphson technique is used in AMPS. To be specific, the solutions to Eqs. (1), (2), and (3) must satisfy the following boundary conditions:

$$\Psi(0) = \Psi_0 - V; \quad \Psi(L) = 0; \quad J_p(0) = -qS_{po}[p_o(0) - p(0)];$$

$$J_p(L) = qS_{pL}[p(L) - p_o(L)]; \quad J_n(0) = qS_{no}[n(0) - n_o(0)];$$

$$J_n(L) = -qS_{nL}[n_o(L) - n(L)].$$

S<sub>po</sub>, S<sub>pL</sub>, S<sub>no</sub>, and S<sub>nL</sub> appearing in those conditions are effective interface recombination speeds for holes and electrons at x = 0 and x = L. In the calculation, we set the interface recombination speed of the left electrode to 1 × 10<sup>5</sup> cm/s and of the right electrode to 1 × 10<sup>7</sup> cm/s.

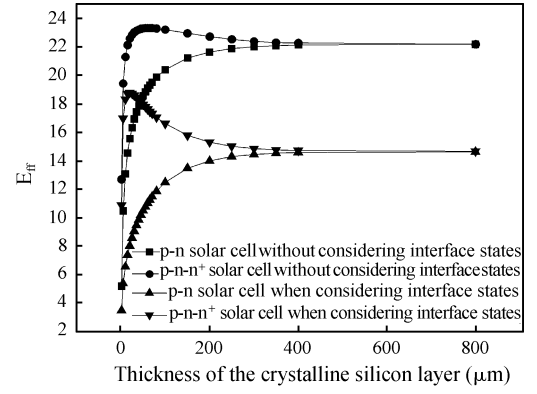


Fig. 2. Efficiency of the p-n and p-n-n<sup>+</sup> solar cells versus the thickness of the c-Si.

### 3. Material parameters

The doping concentrations of the n<sup>+</sup>-a-Si:H layer and the p-a-Si:H layer are 8 × 10<sup>19</sup> and 8 × 10<sup>18</sup> cm<sup>-3</sup>, respectively, and their thicknesses are both 10 nm. The doping concentration of the n-c-Si layer, sandwiched between the n<sup>+</sup>-a-Si:H layer and the p-a-Si:H layer, is 1 × 10<sup>17</sup> cm<sup>-3</sup>, and its thickness is in the range of 1000–8000 000 nm. RF and RB were 0.6 and 1, respectively, and a light trapping structure was not considered in the simulation. The interface state between the p-a-Si:H layer and the n-c-Si layer with a thickness of 1 nm (about 4 atomic layers) is introduced, and its dangling bond state density, which tends to have a double-Gaussian distribution, is in the range of 10<sup>15</sup>–10<sup>19</sup> cm<sup>-3</sup>. From this, the dangling bond state surface density can be estimated to be about 10<sup>8</sup>–10<sup>12</sup> cm<sup>-2</sup>. The electron and hole capture cross sections are 1 × 10<sup>-14</sup> cm<sup>2</sup>, 1 × 10<sup>-15</sup> cm<sup>2</sup> (donor-like) and 1 × 10<sup>-15</sup> cm<sup>2</sup>, 1 × 10<sup>-14</sup> cm<sup>2</sup> (acceptor-like), respectively<sup>[3]</sup>.

The contact between the film and the electrode is ohmic. The material parameters of amorphous and crystalline silicon and the carrier recombination speeds on the interface of the ohmic contact are shown in Table 1. The simulated light is AM 1.5, and its effective wave band is in the range of 0.4–1.1 μm.

### 4. Results and discussions

In Fig. 2, without considering interface states, the p-n-n<sup>+</sup> solar cell efficiency was almost the same as that of the p-n solar cell when the same thickness is larger than 400 μm. In contrast, they were significantly different when the thickness was lower than 400 μm. When taking the interface states into account, the efficiency of the p-n-n<sup>+</sup> solar cell slowly increased when reducing the thickness of the n-c-Si layer. It reached its peak value of 23.671% when the thickness is 65 μm, and then slowly decreased; a rapid reduction of the efficiency was found when the thickness is less than 20 μm. When reducing the thickness of the n-c-Si layer, the efficiency of the p-n solar cell decreases gradually. Compared with the performance of cells with or without interface states, it was found that the interface states had a great impact on the performance of the solar cell, and interface states could reduce the efficiency to a

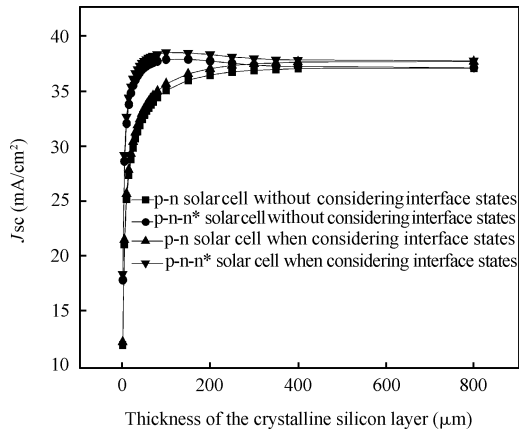


Fig. 3. Short circuit of the p–n and p–n–n<sup>+</sup> solar cells versus the thickness of the c-Si.

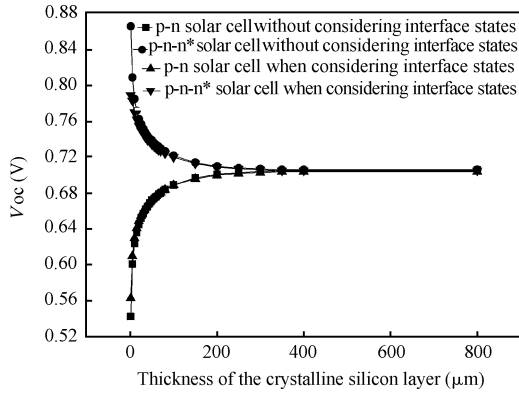


Fig. 4. Open circuit voltage of the p–n and p–n–n<sup>+</sup> solar cells versus the thickness of the c-Si.

large extent. As can be observed, the efficiency difference between p–n and p–n–n<sup>+</sup> cells for the case that interface states are considered was much larger than for the case that does not consider interface states. This indicates that the BSF can effectively inhibit the degradation of the efficiency caused by interface states.

Based on the above-mentioned phenomena, it is considered that photocarriers can easily recombine at an interface state that is equal to a recombination center. This will affect the collection efficiency of photocarriers. Owing to the potential barrier  $\psi_n$  existing between the n layer and the n<sup>+</sup> layer, the minority carriers generated by the low energy photons in the n-region are limited to the lightly doped n-region and cannot diffuse to the recombination center at the interface and at the ohmic contact electrode, where the surface recombination velocity is infinity. In fact, for holes in the n-region,  $\psi_n$  is a potential barrier as long as the thickness of the n-region is much smaller than the diffusion length of the holes ( $W_N \ll L_p$ ). The holes generated by low energy photons in the n-region are not recombined at the back surface of the p–n junction and the recombination centers at the interface, but diffuse to the boundary of the p–n junction. So, the photocarriers are “swept” over the p–n junction, which will enlarge the low energy spectral response.

As shown in Fig. 3, for the same cell (p–n or p–n–n<sup>+</sup>), the impact of interface states on the short circuit current  $J_{sc}$  is very small. In contrast to the cell without interface states, the

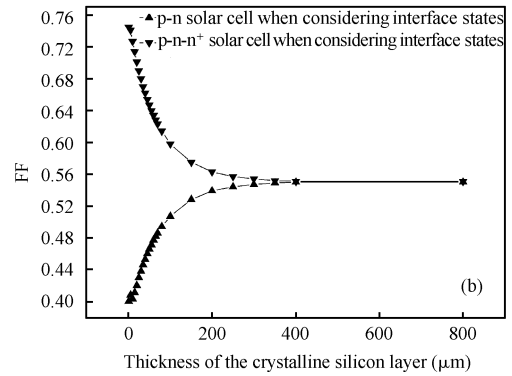
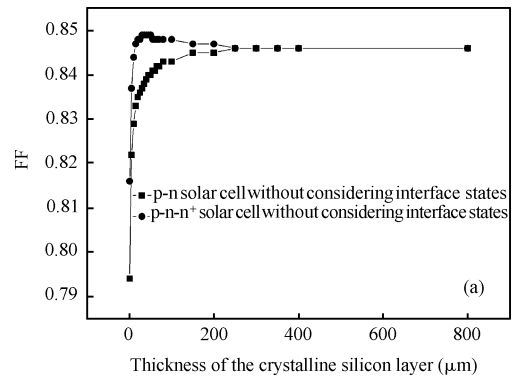


Fig. 5. (a) Fill factor of the p–n and p–n–n<sup>+</sup> solar cell versus the thickness of c-Si without interface states; (b) Fill factor of the p–n and p–n–n<sup>+</sup> solar cell versus the thickness of c-Si with interface states.

cell with interface states has a larger  $J_{sc}$  when the thickness is lower than 200  $\mu\text{m}$ . This result occurred mainly because of the reflective action of minority carriers in the case of a back barrier, therefore, reducing the recombination rate of the back surface, and improving the quantum efficiency of long-wave photons, thus, enlarging  $J_{sc}$ .

In Fig. 4, the open circuit voltage  $V_{oc}$  of the p–n–n<sup>+</sup> solar cell increases with a decreasing thickness of the c-Si layer, which is the reverse behavior to what is seen when using a p–n solar cell. The improvement of  $V_{oc}$  is mainly due to the effect of the BSF. It effectively collects electrons and increases  $V_{oc}$ , when the barrier action of the n–n<sup>+</sup> junction works in the whole n-c-Si layer. So,  $V_{oc}$  increased when decreasing the thickness of the n-c-Si layer. Figure 5 shows the effects of interface states and a back surface field on the fill factor of a solar cell for different thicknesses. As seen in Fig. 5(a), without considering interface states, the fill factor of the p–n solar cell decreased slowly with the thickness of the n-c-Si layer, while the fill factor of the p–n–n<sup>+</sup> solar cell first increased and then decreased. Figure 5(b) shows a monotonic increase of the p–n solar cell’s fill factor with the thickness of the n-c-Si layer. The p–n–n<sup>+</sup> cells show the reversed behavior.

When considering interface states, the fill factor of the p–n structure cell decreased more quickly than for the case without interface states; moreover, if the thickness is less than 400  $\mu\text{m}$ , the fill factor of the p–n–n<sup>+</sup> cell increased monotonously as the thickness of the c-Si layer decreased.

This phenomenon can be explained as follows: Based on the ideal diode model of a solar cell, the fill factor FF is related to the dark current, in case the series resistance can be ignored.

This relation is given by<sup>[4]</sup>

$$FF \approx \left\{ 1 - \frac{1}{\ln(J_{sc}/J_0)} \right\} \left\{ 1 - \frac{\ln[\ln(J_{sc}/J_0)]}{\ln(J_{sc}/J_0)} \right\}. \quad (4)$$

For the p–n cell without considering interface states, if  $J_0$  is unchanged, FF decreases monotonously as  $J_{sc}$  reduces. Some research results indicate that, if the interface state density changed from  $5 \times 10^{11}$  to  $5 \times 10^{12} \text{ cm}^{-2}$ , the dark current increased by almost three orders of magnitude<sup>[5]</sup>. It is shown that the dark current increase by several orders of magnitude is induced by interface states. Compared to the great change of the dark current  $J_0$ ,  $J_{sc}$  is changed very much; in fact, it can even be ignored. So,  $J_{sc}/J_0$  also increases by several orders of magnitude. From Eq. (3), we realize that, if interface states are considered, the fill factor decreases more quickly than without considering interface states in p–n junction cells. In the p–n–n<sup>+</sup> cell, the voltage direction of the n<sup>+</sup>–n junction is opposite to the terminal voltage, thus, reducing the forward bias on the cell. Moreover, the n<sup>+</sup>–n junction can stop minority carriers from diffusing into n<sup>+</sup>-type region or the interface composite center, thus, improving the efficiency and reducing the value of the injected dark current<sup>[6]</sup>. The thinner the cell is, the clearer it is. Without considering interface states, the decreasing value of the dark current is low, mainly because the fill factor is increasing slowly as the c-Si region gets thinning in a p–n–n<sup>+</sup> cell with a back electric field. But, if the cell is too thin to reduce the efficiency, the decrease of  $J_{sc}$  is higher than the decrease of the dark current produced by the back electric field; so, the fill factor is easily decreased. When considering interface states in the case that the thickness of the c-Si region is more than 400  $\mu\text{m}$ , the influence on the cell induced by the back electric field tends can be ignored, while the increase of the dark current produced by  $J_{sc}$  and the interface state is nearly unchanged. So, the thickness of the c-Si region is also almost unchanged if it is larger than 400  $\mu\text{m}$ . When the thickness is less than 400  $\mu\text{m}$ , the back electric field begins to take effect. It can prevent photo-minority carriers from reaching the interface composite centers and effectively reduces the influence of the dark current caused by interface states. The thinner the c-Si region is,

the more effective it is; the cells influenced by interface states are more similar to the ones without interface states with regard to the dark current. Therefore, the fill factors of both are similar. Moreover, the fill factor of the p–n–n<sup>+</sup> cell increases gradually as the thickness of the c-Si region decreases.

## 5. Conclusions

(1) It was shown that interface states had a very important influence on the performance of solar cells. The efficiency of a cell decreased obviously when interface states are present. (2) The BSF had a bigger effect on the photovoltaic performances of thin solar cells than on the performance of thick cells. The BSF of the p–n–n<sup>+</sup> solar cells can effectively inhibit the reduction of the cell performance caused by interface states. (3) According to the theoretical optimization results, we obtained a rather good p–n–n<sup>+</sup> solar cell performances, with a  $J_{sc}$  of 38.101 mA/cm<sup>2</sup>, an EFF of 23.671%, a fill factor of 0.848, and a  $V_{oc}$  of 0.732 V.

## Acknowledgments

We acknowledge the use of the AMPS-1D program developed by Dr. Fonash's group of the Pennsylvania State University.

## References

- [1] Wang S C. The important degree and prospect of photovoltaic power generation in China. The 8th China Photovoltaic Conference, Beijing, 2004: 1
- [2] Sze S M. Physics of semiconductor devices. New York: John Wiley & Sons Press, 1981: 51
- [3] Gall S, Hirschauer R. Spectral characteristics of a-Si:H/c-Si heterostructures. Solar Energy Material & Solar cells, 1997, 49(1–4): 157
- [4] Fahrenbruch A L, Bube R H. Fundamentals of solar cells. New York: Academic Press, 1983: 85
- [5] Hu Z H. Numerical simulation of nc-Si:H/c-Si heterojunction solar cells. Acta Phys Sinica, 2003, 52(1): 217
- [6] An Q L. Principles of solar cell technology. Shanghai: Shanghai Science and Technology Press, 1984: 66